Coherent Light Transport in a Cold Strontium Cloud

Y. Bidel,[1] B. Klappauf,[2] J. C. Bernard,[1] D. Delande,[3] G. Labeyrie,[1] C. Miniatura,[1]
D. Wilkowski,[1,*] and R. Kaiser[1]

[1]*Laboratoire Ondes et Désordre, FRE 2302, 1361 route des Lucioles F-06560 Valbonne, France*
[2]*Optoelectronics Research Center, University of Southampton, SO17 1BJ Southampton, United Kingdom*
[3]*Laboratoire Kastler Brossel, Université Pierre et Marie Curie, F-75252 Paris, France*
(Received 13 March 2002; published 7 May 2002)

We study light coherent transport in the weak localization regime using magneto-optically cooled strontium atoms. The coherent backscattering cone is measured in the four polarization channels using light resonant with a $J_g = 0 \rightarrow J_e = 1$ transition of the strontium atom. We find an enhancement factor close to 2 in the helicity preserving channel, in agreement with theoretical predictions. This observation confirms the effect of internal structure as the key mechanism for the contrast reduction observed with a rubidium cold cloud [G. Labeyrie *et al.,* Phys. Rev. Lett. **83**, 5266 (1999)]. Experimental results are in good agreement with Monte Carlo simulations taking into account geometry effects.

DOI: 10.1103/PhysRevLett.88.203902 PACS numbers: 42.25.Dd, 32.80.Pj

During the past twenty years, the outstanding development of mesoscopic physics led to a critical inspection of coherent effects in wave transport. First motivated by electronic transport in conducting devices [1], the underlying physical ingredients proved to be relevant to any linear waves and in particular to light. This triggered active research in the field of optics during the past two decades [2], leading to the observation of coherent backscattering enhancement [3] and universal conductance fluctuations [4], to quote a few. A challenge in this field is still the observation of strong localization of visible light. It was recently reported for near-infrared light using semiconductors powders [5], but the interpretation of the experiment in term of Anderson localization was questioned [6]. Cold atoms have been quite recently considered as promising scattering media to achieve strong localization [7]. Indeed, they constitute perfectly monodisperse samples of resonant point–dipole scatterers with large cross sections. Moreover high spatial density is achieved by adequate trapping techniques [8,9].

In this Letter we report the observation of coherent backscattering (CBS) of light on cold strontium atoms in the weak localization regime $kl \gg 1$ (k is the light wave number and l is the elastic mean-free path). CBS is an interferential enhancement of the *average* scattered intensity reflected off a disordered scattering medium [10]. It originates from a two-wave constructive interference near exact backscattering between waves traveling along a given scattering path and its reversed counterpart. For classical scatterers, bearing on general symmetry arguments valid in the absence of any magnetic field, the CBS interfering amplitudes have been shown to have equal weights at exact backscattering in the so-called parallel polarization channels [11]. In the lin $\parallel$ lin (linear $\parallel$ linear) channel the incoming and detected light fields have the same linear polarization. In the h $\parallel$ h (helicity $\parallel$ helicity) channel, both light fields are circularly polarized with the same helicity, that is opposite polarizations (because the CBS signal is emitted in the backward direction). In the perpendicular channels, nothing ensures the equality of the two interfering amplitudes, and the contrast of the interference is decreased. Single scattering events require a separate treatment as direct and reversed paths coincide in the backward direction and do not contribute to the CBS enhancement. For spherically symmetric scatterers, single scattering does not contribute in the lin $\perp$ lin and h $\parallel$ h channels. Thus, the CBS contrast (peak-to-background ratio) is predicted and has been observed to be exactly 2 in the helicity preserving polarization channel h $\parallel$ h [12]. By using an atomic gas at resonance, a dynamic breakdown of the CBS effect can occur due to the scatterers motion during the transit time of a photon inside the medium. This restricts the rms velocity δv below a critical velocity given by $v_c = \Gamma/k$ (where Γ is the width of the atomic dipole resonance), a condition which is well fulfilled for a laser cooled atomic gas [13]. The quantum internal structure of atoms also has severe consequences for coherent light transport in atomic media. A degeneracy in the ground state induces a dramatic reduction of the CBS interference [14]. This has first been experimentally observed with a cold rubidium sample on a $J_g = 3 \rightarrow J_e = 4$ transition [13]. These results highly motivated the use of nondegenerate ground state atoms, such as strontium, to benefit from full interference effects in coherent transport.

The cold strontium (Sr) cloud is stored in a magneto-optical trap (MOT). The transverse velocity of an effusive atomic beam, extracted from a 500 °C oven, is immediately compressed with 2D optical molasses. A 27-cm-long Zeeman slower then reduces the longitudinal velocity to within the capture velocity range of the MOT ($\sim$50 ms^{-1}). The Zeeman slower, molasses, MOT, and probe laser beams at 461 nm are generated from the same frequency-doubled source. Briefly, a single-mode grating-stabilized diode laser and a tapered amplifier are used in a master-slave configuration to produce 500 mW at 922 nm. The infrared light is then frequency

doubled in a semimonolithic standing wave cavity with an intracavity $KNbO_3$ crystal. The cavity is resonant for the infrared light while the second harmonic exits through a dichroic mirror providing 150 mW of tunable single-mode light, which is then frequency locked onto the 461 nm $^1S_0$-$^1P_1$ strontium line in a heat pipe. We use acoustooptic modulators for subsequent amplitude and frequency variations. The MOT is made of six independent trapping beams of 5.2 mW cm^{-2} each, red detuned by $\delta = -\Gamma$ from the resonance. The saturation intensity is 42.5 mW cm^{-2} and the natural width of the transition is $\Gamma/2\pi = 32$ MHz. Two anti-Helmholtz coils create a 100 G cm^{-1} magnetic field gradient to trap the atoms. A small population loss to metastable states is repumped to the ground state using two additional red lasers. The best achieved optical thickness of our Sr MOT is $b \approx 3$. It is deduced from transmission measurements of a resonant probe through the cloud shortly after switching off the MOT. Note that, because the optical thickness of the atomic cloud is larger than one, the imaging of the cloud does not yield a signal proportional to the atomic density and the whole process thus overestimates the size of the cloud (see discussion below). The number of trapped atoms $N \simeq 10^7$ is derived from the MOT fluorescence signal. From a CCD image the rms radius of the cloud has been estimated at 0.65 mm. Since the mean-free path is $l = 1/(n\sigma)$ (n being the atomic density and $\sigma = 6\pi/k^2$ being the resonant light scattering cross section), this yields $l \approx 0.5$ mm (or $kl \simeq 7000$). The rms velocity of the atoms is about 1 ms^{-1}, well below the critical velocity $v_c = 15$ ms^{-1}.

The detailed experimental procedure for the CBS observation has been published elsewhere [13]. For the Sr experiment, the signal is obtained using a collimated resonant probe beam with a waist of 3 mm. To avoid any effects linked to the saturation of the optical transition (nonlinearities, inelastic radiation spectrum) [15], the probe intensity is weak (saturation parameter $s = 0.02$). The scattered light is collected in the backward direction by placing a CCD camera in the focal plane of an achromatic doublet. The angular resolution of our apparatus is 0.1 mrad, roughly twice the CCD pixel angular resolution. To avoid recording the MOT fluorescence signal while recording the CBS signal, a time-sequenced experiment is developed. The trapping beams and the magnetic field gradient are switched off during the CBS acquisition sequence (duration 100 μs) and then switched on to recapture the atoms (duration 95% of the 6 ms total cycle time). This procedure also eliminates any possible unwanted nonlinear wave mixing processes. The whole time sequence is then repeated as long as necessary for a good signal-to-noise ratio (typically 15 min in the experiment). During the CBS sequence, the image field is opened (and then closed during the MOT sequence) thanks to a mechanical chopper. During the CBS probe interaction time, each atom scatters about 200 photons on average but always remains in resonance since the mean atomic velocity increase is far below v_c. Consequently, most of them are recaptured during the following MOT sequence. The CBS images (see Fig. 1) are finally obtained by subtracting the background image taken without cold atoms. This background image is recorded in the absence of the magnetic gradient during all the acquisition time. We thus checked that the fluorescence signal from the residual Sr atoms was negligible.

In the helicity preserving channel (h $\|$ h), the enhancement factor is found to be $\alpha = 1.86 \pm 0.10$ with an optical thickness of $b = 2.9$ (see Fig. 2), slightly lower than the theoretical prediction $\alpha = 2$. Several experimental issues can explain the difference. The finite angular resolution of the detection apparatus lowers the CBS enhancement factor by an amount evaluated to $\delta\alpha \approx 0.06$. Because single scattering contributes more than 90% of the total signal in the two authorized channels (see Table I), the reduction of the cone contrast due to imperfect polarization channel isolation in the h $\|$ h is not negligible. We have measured, in the limit of low optical thickness where single scattering dominates over multiple scattering, the fraction of detected light in the forbidden h $\|$ h channel with respect to the total scattered light. We found a channel isolation about 5×10^{-4} leading to a reduction of $\delta\alpha \approx 0.03$. Note that single scattering depolarization

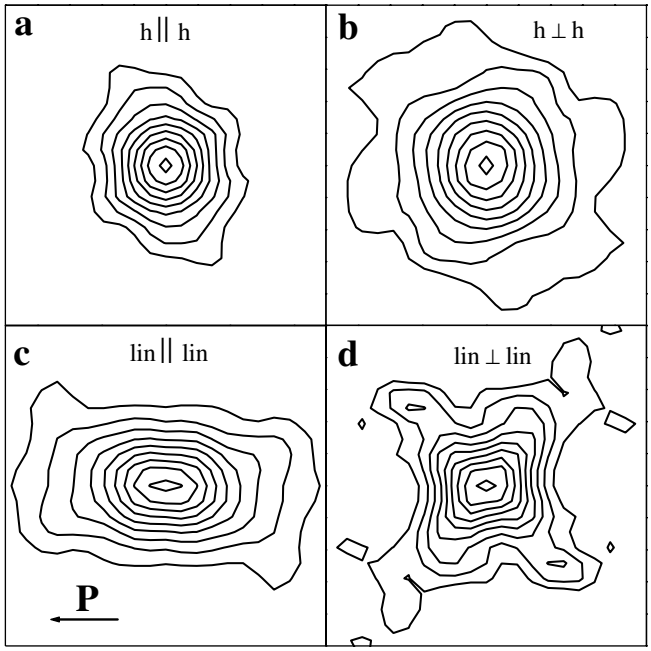

FIG. 1. Isocontours of the coherent backscattering cones obtained on a cloud of cold strontium atoms in the four polarization channels. We plot the CBS signal after subtraction of the large angle background, as a function of the backscattering angle. All cone heights have been scaled to 1. For better signal/noise the images have been symmetrized. The total angular range is 1 mrad. The lowest isocontour corresponds to roughly 20% of the peak intensity. For the linear channels, the incident polarization is horizontal.

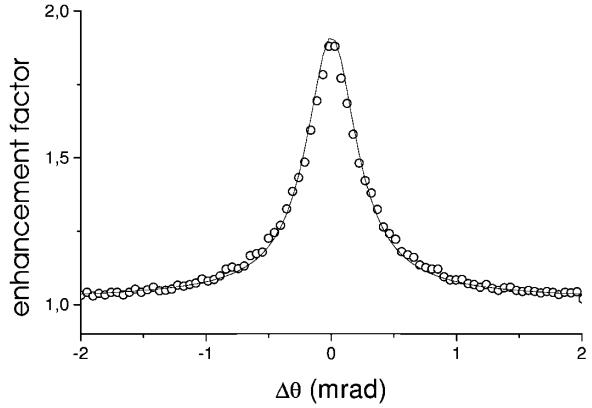

FIG. 2. Angular scan of the CBS cone for the h ∥ h polarization channel. The optical thickness is $b = 2.9$. The experimental data are represented by open circles. For better signal/noise we perform an angular averaging of the original image. The solid line is the result of a Monte Carlo calculation taking into account the geometry of the atomic cloud (Gaussian distribution of the atomic density with rms radius value 0.45 mm) and experimental imperfections like the polarization channel isolation and angular resolution effects. The agreement is clearly excellent. The measured width of the cone is $\Delta\theta_{\mathrm{CBS}} = 0.50 \pm 0.04$ mrad.

induced by a stray magnetic field acts here like an imperfect polarization isolation. For this reason, its impact on the cone reduction has been minimized during the channel isolation procedure. Another possible source of contrast reduction is a Faraday effect induced by the residual magnetic field [16]. It turns out that, despite the huge Verdet constant in the atomic gas medium [17], its effect should be smaller than those previously discussed. We also checked that the finite transverse size of the laser beam has no significant influence on the signal. Taking into account the systematic errors, we find that the CBS enhancement factor should rather be $\alpha = 1.91$, consistent with the measured value. A remaining (but yet uncontrolled) source of error in determining α is certainly an imperfect estimation of the background level where the CBS interference has vanished, i.e., measured at angles large compared to the cone width $\theta \gg \Delta\theta_{\mathrm{CBS}}$.

TABLE I. Comparison between the CBS enhancement factor and peak width measured in the experiment with the results of a Monte Carlo calculation, for optical thickness $b = 2$. In each polarization channel, the experimental enhancement factor α is given with a $\pm 2\sigma$ error bar. For linear polarization channels, the $\Delta\theta_{\mathrm{CBS}}$ values are given only for scans parallel to the incident polarization. The results of MC simulation (noted MC) are given for a Gaussian distribution of the cloud with a rms radius value 0.45 mm. The experimental imperfections, such as the polarization channel isolation and angular resolution effects, have been taken into account in the MC simulation values noted MC*. The "Background" column shows the relative contribution of the channel to the total large angle scattered intensity in the backward direction.

Channel		Background	α	$\Delta\theta_{\mathrm{CBS}}$ (mrad)
h ∥ h	Exp.	7.5%	1.77 ± 0.13	0.52 ± 0.07
	MC	7.8%	2	0.48
	MC*	7.8%	1.87	0.52
h⊥h	Exp.	92.5%	1.17 ± 0.03	0.71 ± 0.10
	MC	92.2%	1.20	0.69
	MC*	92.2%	1.19	0.75
lin ∥ lin	Exp.	96.0%	1.17 ± 0.03	0.9 ± 0.2
	MC	95.5%	1.24	0.92
	MC*	95.5%	1.22	0.98
lin⊥lin	Exp.	4.0%	1.59 ± 0.20	0.5 ± 0.3
	MC	4.5%	1.74	0.48
	MC*	4.5%	1.62	0.49

In the other polarization channels, we observe lower enhancement factors as predicted by the theory (see Table I). In the lin ∥ lin and h⊥h channels, the small enhancement factors are mainly due to the strong single scattering contribution (see the relative large angle background values given in Table I), which is very important since the optical thickness is not very large. In the lin⊥lin channel (where single scattering is absent), the relatively high contrast value is explained by the low optical thickness. Indeed, in this situation, short scattering paths dominate and double scattering is known to exhibit full interference contrast in all polarization channels [18]. In Table I, we also show data obtained with a Monte Carlo (MC) calculation, where the amplitude of a multiple scattering path is computed as a function of the initial and final polarizations and of the geometrical positions of the various scatterers. We use a Gaussian distribution for the spatial density of scatterers and take into account the spatial variations of the mean-free path during the photon propagation. Our numerical method is tantamount to computing the integral involved in the configuration average using a MC procedure. Given a spatial configuration of the scatterers, we compute simultaneously the various scattering contributions at different scattering orders using the "partial photon" trick [19]. Typically, it is enough to launch less than one million photons on the medium to get a good signal/noise ratio for the CBS peak. For all polarization channels, there is a good agreement for the cone height between experiments and MC simulations adjusted to take into account the polarization channel isolation and angular resolution effects.

The experimental values $\Delta\theta_{\mathrm{CBS}}$ of the FWHM CBS angular cone width are systematically higher (by a factor 1.4) than the ones given by the MC simulation using the measured optical thickness b and the size of the atomic cloud. As discussed above, our experimental procedure slightly overestimates the size of the cloud. Modifying the size of the cloud (keeping b constant) results only in a global multiplication of the angular scale, keeping both the enhancement factor and the cone shape identical. We are thus inclined to think that the actual rms radius of the cloud is $\approx$0.45 mm instead of 0.65 mm. With this corrected value, we observe excellent agreement between MC and the experimental data *in all polarization channels*

(see Fig. 2 and Table I). The angular dependence of the cone shape in the linear channels reflects the anisotropy of the scatterer's pattern [18]. In the lin $\parallel$ lin channel, an elliptical shape with the major axis parallel to the incident polarization is predicted and indeed observed (Fig. 1c). In the lin $\perp$ lin channel, the directions of maximum scattering are tilted at 45° from the incident polarization, yielding a "cloverleaf" CBS cone shape (Fig. 1d).

To summarize, we measured the coherent backscattering cone in four different characteristic polarization channels. Our results are in good agreement with a Monte Carlo calculation. The restoration of a full interference contrast in coherent multiple scattering with atomic gases (as exemplified by the maximum enhancement factor of 2 obtained in the helicity preserving channel) has interesting potentialities for wave localization experiments with cold atoms. For example, in the quest for Anderson localization (which could be obtained only at high density where $kl \approx 1$) where interferences play a crucial role, a $J_g = 0 \rightarrow J_e = 1$ transition appears to be a good choice, since a degenerate internal structure is known to reduce the interference significantly [14]. A maximum enhancement factor of 1.2 was found in a Rb experiment [13]. Is it now possible to increase the cloud density to reach the Anderson localization threshold? For this purpose, cooling strontium with the intercombination line in a dipole trap appears to be a promising technique [8].

The authors thank the CNRS and the PACA region for their financial support. Laboratoire Kastler Brossel is laboratoire de l'Université Pierre et Marie Curie et de l'Ecole Normale Supérieure, UMR 8552 du CNRS.

*Electronic address: wilkowsk@inln.cnrs.fr
URL: http://www-lod.inln.cnrs.fr/

[1] D. K. Ferry and S. M. Goodnick, *Transport in Nanostructures* (Cambridge University Press, New York, 1997); S. Datta, *Electronic Transport in Mesoscopic Systems* (Cambridge University Press, Cambridge, 1995).

[2] V. L. Kuz'min and V. P. Romanov, Phys. Usp. **39**, 231 (1996); M. C. W. van Rossum and Th. M. Nieuwenhuizen, Rev. Mod. Phys. **71**, 313 (1999).

[3] P. E. Wolf and G. Maret, Phys. Rev. Lett. **55**, 2696 (1985); M. P. Van Albada, and A. Lagendijk, Phys. Rev. Lett. **55**, 2692 (1985).

[4] F. Scheffold and G. Maret, Phys. Rev. Lett. **81**, 5800 (1998).

[5] D. S. Wiersma, P. Bartolini, A. Lagendijk, and R. Righini, Nature (London) **390**, 671 (1997).

[6] F. Scheffold, R. Lenke, R. Tweer, and G. Maret, Nature (London) **398**, 207 (1999).

[7] Th. M. Nieuwenhuizen, A. L. Burin, Yu. Kagan, and G. V. Shlyapnikov, Phys. Lett. A **184**, 360 (1994).

[8] T. Ido, Y. Isoya, and H. Katori, Phys. Rev. A **61**, R061403 (2000); H. Katori, T. Ido, and M. Gonokami, J. Phys. Soc. Jpn. **68**, 2479 (1999).

[9] *Ultracold Atoms and Bose-Einstein Condensation,* edited by K. Burnett, OSA Trends in Optics and Photonics Series Vol. 7 (Optical Society of America, Washington, D.C., 1996).

[10] E. Akkermans, P. E. Wolf, R. Maynard, and G. Maret, J. Phys. (Paris) **49**, 77 (1988).

[11] B. A. van Tiggelen and R. Maynard, in *Wave Propagation in Complex Media,* edited by G. Papanicolaou, IMA Volumes in Mathematics and its Applications Vol. 96 (Springer, New York, 1997), p. 252.

[12] D. S. Wiersma, M. P. van Albada, B. A. van Tiggelen, and A. Lagendijk, Phys. Rev. Lett. **74**, 4193 (1995).

[13] G. Labeyrie, F. de Tomasi, J. C. Bernard, C. A. Müller, C. Miniatura, and R. Kaiser, Phys. Rev. Lett. **83**, 5266 (1999); G. Labeyrie, C. Müller, D. Wiersma, C. Miniatura, and R. Kaiser, J. Opt. B: Quantum Semiclassical Opt. **2**, 672 (2000).

[14] T. Jonckheere, C. A. Müller, R. Kaiser, C. Miniatura, and D. Delande, Phys. Rev. Lett. **85**, 4269 (2000); C. A. Müller, T. Jonckheere, C. Miniatura, and D. Delande, Phys. Rev. A **64**, 053804 (2001).

[15] V. M. Agranovich and V. E. Kravtsov, Phys. Rev. B **43**, 13 691 (1991); A. Heiderich, R. Maynard, and B. van Tiggelen, Opt. Commun. **115**, 392 (1995).

[16] R. Lenke and G. Maret, Eur. Phys. J. B **17**, 171 (2000).

[17] G. Labeyrie, C. Miniatura, and R. Kaiser, Phys. Rev. A **64**, 033402 (2001).

[18] M. P. van Albada, M. B. van der Mark, and A. Lagendijk, Phys. Rev. Lett. **58**, 361 (1987).

[19] R. Lenke and G. Maret, in *Scattering in Polymeric and Colloidal Systems,* edited by W. Brown and K. Mortensen (Gordon and Breach, Reading, 2000), pp. 1–72.